Effect of 3-Bromopyruvate and Atovaquone on Infection during *In Vitro* Interaction of *Toxoplasma gondii* and LLC-MK2 Cells

Loyze Paola O. de Lima,[a,b] Sergio H. Seabra,[b] Henrique Carneiro,[a] Helene S. Barbosa[a]

Laboratório de Biologia Estrutural, Instituto Oswaldo Cruz, Fiocruz, Manguinhos, Rio de Janeiro, Brazil[a]; Laboratório de Tecnologia em Bioquímica e Microscopia, Centro Universitário Estadual da Zona Oeste (UEZO), Campo Grande, Rio de Janeiro, Brazil[b]

Toxoplasma gondii infection can be severe during pregnancy and in immunocompromised patients. Current therapies for toxoplasmosis are restricted to tachyzoites and have little or no effect on bradyzoites, which are maintained in tissue cysts. Consequently, new therapeutic alternatives have been proposed as the use of atovaquone has demonstrated partial efficacy against tachyzoites and bradyzoites. This work studies the effect of 3-bromopyruvate (3-BrPA), a compound that is being tested against cancer cells, on the infection of LLC-MK2 cells with *T. gondii* tachyzoites, RH strain. No effect of 3-BrPA on host cell proliferation or viability was observed, but it inhibited the proliferation of *T. gondii*. The incubation of cultures with lectin *Dolichos biflorus* agglutinin (DBA) showed the development of cystogenesis, and an ultrastructural analysis of parasite intracellular development confirmed morphological characteristics commonly found in tissue cysts. Moreover, the presence of degraded parasites and the influence of 3-BrPA on endodyogeny were observed. Infected cultures were alternatively treated with a combination of this compound plus atovaquone. This resulted in a 73% reduction in intracellular parasites after 24 h of treatment and a 71% reduction after 48 h; cyst wall formation did not occur in these cultures. Therefore, we conclude that the use of 3-BrPA may serve as an important tool for the study of (i) *in vitro* cystogenesis; (ii) parasite metabolism, requiring a deeper understanding of the target of action of this compound on *T. gondii*; (iii) the alternative parasite metabolic pathways; and (iv) the molecular/cellular mechanisms that trigger parasite death.

Toxoplasma gondii is an obligatory intracellular protozoan causative agent of toxoplasmosis that has a life cycle involving members of the family *Felidae* as definitive hosts and warm-blooded animals, including humans, as intermediate hosts (1). The development of toxoplasmosis involves asexual replication. This gives rise to tachyzoites that are characterized by rapid growth during acute infection and bradyzoites found within tissue cysts, which slowly multiply and are responsible for the chronic phase of toxoplasmosis (2). In humans, the disease is typically asymptomatic; however, it is severe in immunocompromised individuals and congenital cases. For control of the infection, the most widely used therapy has been a combination of pyrimethamine and sulfadiazine (3), but this combination is commonly associated with several limitations due to adverse reactions, hypersensitivity, and hematologic toxicity (4). Although this combination is the treatment of choice and is used as prophylaxis, some patients are intolerant to this scheme and require alternative therapies (5). Atovaquone, a hydroxyl-1,4-naphthoquinone with a broad spectrum of antiprotozoan activity, has been FDA approved for the treatment of toxoplasmosis. This compound has shown efficacy against tachyzoites *in vitro* and *in vivo* (6, 7) and has a synergistic effect with clindamycin in acute murine toxoplasmosis (8).

In this study, we analyzed the effect of the pyruvic acid analogue 3-bromopyruvate (3-BrPA), which proved to be a potent inhibitor of ATP synthesis, inhibiting the proliferation of cancer cells without apparent toxicity or recurrence (9–11). The enzyme hexokinase II was the first reported target of 3-BrPA (12), but this alkylating agent selectively inhibits mitochondrial oxidative phosphorylation, angiogenesis, and energy production in cancer cells (13, 14). The enzyme glyceraldehyde-3-phosphate dehydrogenase (GAPDH) is also inhibited by 3-BrPA in human hepatocellular carcinoma cell lines (15), leading to death by apoptosis (16).

In microorganisms, 3-BrPA inhibits the proliferation of differ-

ent strains of *Saccharomyces cerevisiae* with an MIC of 1.8 mM (17) and of the human pathogen *Cryptococcus neoformans* with an MIC of 120 mM (18). In protozoa such as *Trypanosoma brucei*, 3-BrPA has inhibitory effects on (i) the motility of the parasite at 13.4 mM and (ii) the efflux of pyruvate at 5.6 mM due to blockage of GAPDH, leading the reduced parasite viability (19, 20).

These data prompted us to study the activity of 3-BrPA on the intracellular development of *T. gondii* in LCC-MK2 cells.

MATERIALS AND METHODS

All procedures were carried out in accordance with the guidelines established by the Colégio Brasileiro de Experimentação Animal (COBEA), by Fundação Oswaldo Cruz, Fiocruz, Committee of Ethics for the Use of Animals (license CEUA LW 50/14), and by the Guidelines on the Care and Use of Animals for Experimental Purposes and Infectious Agents (NACLAR).

Cell culture. The epithelial cell line LLC-MK2 (ATCC CCL7), isolated from the kidney of the rhesus monkey, *Macaca mulatta*, was grown in Dulbecco's modified Eagle medium (DMEM) supplemented with 5% fetal bovine serum (FBS) and maintained at 37°C in a 5% CO_2 atmosphere. Subcultures were performed via enzymatic cell dissociation in 0.25% trypsin. After dissociation, the cells were placed in culture medium at 4°C

with 10% FBS to inhibit the action of trypsin. The isolated cells were centrifuged for 7 min at $650 \times g$ at 4°C, and the cells were grown in new bottles. This procedure was repeated when cells reached a confluence of ~90% that occurred on average every 48 h.

Parasites. Tachyzoites of *T. gondii*, RH strain, were maintained in CF1 mice via serial intraperitoneal inoculation of 10^5 to 10^6 parasites per mouse in phosphate-buffered saline (PBS). After 48 to 72 h, parasites were harvested via peritoneal lavage using PBS, pH 7.2, and centrifuged at $200 \times g$ for 5 min to remove blood cells and cell debris. The supernatant containing tachyzoites was collected and centrifuged again at $1,000 \times g$ for 10 min. The final pellet was resuspended in DMEM, quantified in a Neubauer chamber, and used in experimental assays.

Evaluation of the effect of compounds on proliferation of LLC-MK2 cells. A 3-BrPA solution at 15 μM concentration was prepared in DMEM, pH 7.4. A stock solution of atovaquone (1 mg/ml) was prepared in a mixture of ethanol and acetone (1:1) and diluted to 100 nM with the culture medium. LLC-MK2 cells were plated and maintained in DMEM supplemented with 5% FBS and treated with 10 μM 3-BrPA or 50 nM atovaquone for 24 h, 48 h, or 6 days. The cells were fixed in 4% paraformaldehyde in PBS, stained with 10% eosin methylene blue in the same buffer, dehydrated in different concentrations of acetone-xylene, and mounted with Entellan. The material was examined under an Axioplan Zeiss light microscope to evaluate the cell proliferation rate, from 10 total fields per coverslip, in duplicate. Other cultures maintained under identical experimental conditions were collected, and cell viability was assessed using 0.4% trypan blue exclusion assay, with 200 total cells per coverslip.

Evaluation of the effect of compounds on proliferation of *T. gondii* in LLC-MK2 cells. The LLC-MK2 cells were plated and infected for 1 h with tachyzoites of *T. gondii*, RH strain, and washed with PBS. Then the cultures were treated with 3-BrPA (1, 2.5, 10, and 15 μM), atovaquone (1, 10, 50, and 100 nM), or 3-BrPA (10 μM) and atovaquone (50 nM) in combination. Treatment was extended for 24 h, 48 h, or 6 days. After treatment, the cultures were fixed, stained, and mounted as described above. Stained cultures were examined under an Axioplan Zeiss light microscope to verify parasitic cell proliferation, considering 200 total cells in duplicate under three independent experimental conditions.

Monitoring of cystogenesis *in vitro*. The LLC-MK2 cells infected with *T. gondii* tachyzoites, RH strain, after treatment were washed and analyzed using fluorescence microscopy. The differentiation of intracellular parasites was monitored using stage-specific antibodies and lectin. Tachyzoites were identified via immunostaining with anti-P30 antibodies, and cysts of *T. gondii* were identified with lectin *Dolichos biflorus* agglutinin (DBA) conjugated to fluorescein isothiocyanate (FITC), which binds to *N*-acetylgalactosamine (GalNAc) groups (19). Initially, the cultures were fixed with 4% paraformaldehyde in PBS for 10 min at 4°C, washed three times for 10 min in PBS, and then incubated for 30 min in 50 mM ammonium chloride to block free aldehyde radicals. After these steps, the cells were permeabilized for 20 min with a PBS solution containing 0.05% Triton X-100 and 4% bovine serum albumin (BSA) to block nonspecific binding.

For the indirect immunofluorescent assays, the host cells were incubated for 2 h at 37°C with an anti-P30 primary antibody diluted 1:100 in PBS-4% BSA. Then the cells were washed with PBS containing 4% BSA and incubated for 1 h at 37°C in the secondary antibody (anti-mouse IgG conjugated to Alexa Fluor 546) at a dilution of 1:600 in PBS-4% BSA. The cells were observed with a confocal laser microscope (LSM 710; Zeiss) at the Centro Universitário Estadual da Zona Oeste. Controls were performed by omitting the primary antibody.

For direct fluorescence, the cells were incubated for 1 h at room temperature with lectin DBA-FITC (1:200 dilution) in PBS-4% BSA. Control for DBA reaction was performed by a competitive reaction with the addition of 50 mM GalNAc. Next, the cells were washed and mounted with Prolong Gold antifade reagent with DAPI (4′,6-diamidino-2-phenylindole; Invitrogen). Analysis of cystogenetic establishment was carried out

by monitoring 200 total infected cells per coverslip in three independent experiments, in duplicate, using a confocal laser microscope (LSM 710; Zeiss). This methodology is based on vacuoles with labeling for DBA-FITC, which has a high affinity for the cyst wall.

Analysis of the effect of 3-BrPA on *T. gondii* infection in LLC-MK2 cells using scanning electron microscopy (SEM). Coverslips containing adhered infected LLC-MK2 cells were fixed for 1 h in 4% recently prepared formaldehyde plus 2.5% glutaraldehyde in 0.1 mM Na cacodylate buffer (pH 7.4) and postfixed for 30 min at room temperature with a solution of 1% OsO_4 in the same buffer. The cells were dehydrated in an ascending acetone series and dried using the critical point method with CO_2. The monolayer was gently scraped off with adhesive tape (22) to expose the internal organization of vacuoles (23). The samples were mounted on aluminum stubs, coated with a 25-nm layer of gold, and examined using a Jeol JSM-6490lV SEM (Tokyo, Japan) at the Centro Universitário Estadual da Zona Oeste.

Analysis of the effect of 3-BrPA on *T. gondii* infection in LLC-MK2 cells using transmission electron microscopy (TEM). LLC-MK2 cells infected with *T. gondii* (treated or not with 3-BrPA) were washed in Ringer solution, fixed with 2.5% glutaraldehyde in 0.1 M Na cacodylate buffer, pH 7.4, and postfixed with 1% OsO_4 in the same buffer. The cells were then dehydrated in graded acetone and embedded in an epoxy resin (PolyBed 812). Ultrathin sections (60 nm) were stained with uranyl acetate and lead citrate and examined with TEM (Jeol JSM-1011) at the Rudolf Barth Electron Microscopy Platform of the Oswaldo Cruz Institut, Fiocruz.

Statistical analysis. The percentage of infection was quantified after 24 to 96 h using 200 cells per coverslip in three independent experiments performed in duplicate and analyzed by two independent observers. The analysis was performed using an Axioplan 2 Zeiss microscope. Quantitative data were expressed as the means ± standard error, and the results were statistically analyzed using the Student-Newman-Keuls test. The differences were considered statistically significant when the *P* values were <0.05.

RESULTS

Effect of 3-BrPA and atovaquone on the proliferation of LLC-MK2. Aiming to ensure that 3-BrPA and atovaquone do not compromise the viability of LLC-MK2 cells, assays were performed using a maximum concentration of 10 μM 3-BrPA and 50 nM atovaquone. The strategy used varied the exposure time of the cells to the compound for comparison with untreated cultures, considering the proliferative capacity of these cells. No interference by the compounds on the proliferation of LLC-MK2 cells was seen between 24 h and 6 days. Thus, under the experimental conditions used in this study, cell viability tested by trypan blue staining remained at >93% at different treatment times (data not shown).

Effect of compound 3-BrPA on the proliferation of *T. gondii*, RH strain, in LLC-MK2 cells. Control cultures were initially infected with *T. gondii* tachyzoites at a parasite-to-host cell ratio of 3:1 for 1 h, washed in Ringer solution, and cultured for 24 h. After 1 h of infection, other cultures were treated for 24 h with 1, 2.5, 10, or 15 μM 3-BrPA. The results showed that regardless of the treatment schedule with 3-BrPA, there were no significant differences in the percentages of infected cells (Fig. 1A). An analysis of the number of parasites per 200 cells showed that the treated cells had fewer intracellular parasites, with an inhibition of ~42%, up 10 μM (Fig. 1B).

Based on these results, we decided to examine the effect of 3-BrPA at 10 μM concentration, which was effective in reducing the number of intracellular parasites. Cultures infected for 1 h in a ratio of 5:1 parasites per host cell and treated for 24 and 48 h showed a significant reduction ($P \leq 0.05$) in the percentage of
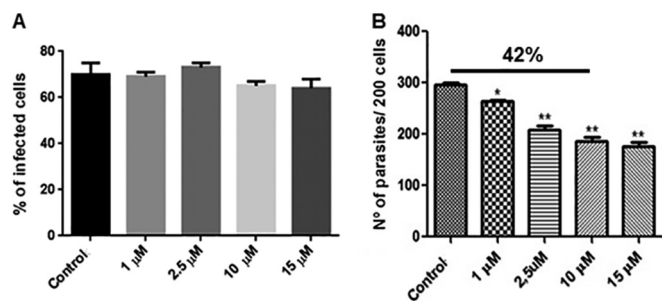
FIG 1 Effect of 3-BrPA on the percentage of LLC-MK2 cells infected with *T. gondii* (A) and the number of intracellular parasites (B). *, $P \leq 0.05$; **, $P \leq 0.01$.

FIG 2 Effect of 3-BrPA on the interaction of *T. gondii*, RH strain, tachyzoites and LCC-MK2 cells. Cultures were maintained under treatment with 10 mM 3-BrPA after 24 and 48 h of infection. The percentage of infected cells (A) and the number of intracellular parasites (B) are shown. *, $P \leq 0.05$.

infected cells after only 48 h of interaction, with an inhibition of 15% compared with that of the control (Fig. 2A). We observed a reduction in the number of parasites after 24 and 48 h by 55% and 61%, respectively, compared to that in the control without the compound (Fig. 2B).

Cultures of LLC-MK2 cells infected at a parasite-to-host cell ratio of 5:1 were kept untreated as an infected control. After 24 h of interaction, parasitophorous vacuoles contained tachyzoites in the form of rosettes for the majority of infected cells (Fig. 3A). However, when cultures were treated with 10 μM 3-BrPA, there were fewer infected cells and vacuoles with only two parasites each (Fig. 3B).

After 48 h, infected cultures maintained as controls showed parasitophorous vacuoles with rosette characteristics and various infected cells (Fig. 3C). Cultures maintained under treatment with 3-BrPA showed few infected cells (Fig. 3D).

Six days postinfection, cultures maintained without treatment showed vacuoles containing large numbers of parasites and several lysed cells with the release of parasites in extracellular medium (Fig. 3E). In contrast, in cultures treated with 3-BrPA, parasitophorous vacuoles with large amounts of unorganized parasites were observed. These had very similar characteristics to those found in tissue cysts, namely, vacuoles containing various parasites and an increased thickness of the membrane surrounding the parasites, consistent with the morphological characteristics of the cyst wall (Fig. 3F). An analysis of the percentage of infected cells showed that there was a significant reduction ($P \leq 0.05$) of 21% in the treated cultures (data not shown).

Ultrastructural evaluation by SEM of the effect of 3-BrPA on intracellular *T. gondii* tachyzoite forms in LLC-MK2 cells. Ultrastructural studies of LLC-MK2 cells infected for 6 days with *T. gondii* tachyzoites showed the presence of parasites in rosettes in parasitophorous vacuoles, a peculiar characteristic of the tachyzoite multiplication process (Fig. 4A). However, after treatment with 3-BrPA, a high quantity of disorganized parasites was found in vacuoles in structures similar to tissue cysts (Fig. 4B and C).

Ultrastructural evaluation by TEM of the effect of 3-BrPA on the interaction of *T. gondii* in LLC-MK2 cells. In control cultures, we observed cells containing parasites in pairs, indicative of recent infection and cell division, presenting good ultrastructural preservation (Fig. 5A). After 6 days of treatment with 10 μM 3-BrPA, we observed a high incidence of cells containing vacuoles with multiple parasites at different stages of differentiation and ultrastructural preservation. Structural damage was more evident,
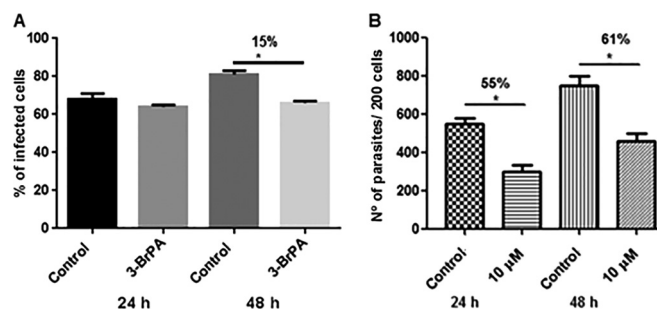
showing highly vacuolated parasites, the concomitant incidence of parasites in typically asynchronous cell division, and the presence of bradyzoites inside the vacuole, which was characterized by electron-dense rhoptries (Fig. 5B). Vacuoles containing anomalous structures were also observed primarily during endodyogeny. Large masses, most likely the source of the residual body, containing two or more nuclei (N) of different sizes in a matrix with various organelles and vesicles were observed; in addition to these structures, we observed parasites with morphological signs consistent with cell death (i.e., vacuolization, shape change) or in the process of cell division by endodyogeny (Fig. 5C). Another notable observation was the presence of vacuoles containing parasites with morphological features similar to those of bradyzoites, especially the presence of amylopectin granules. An associated accumulation of electron-dense material in the inner face of the parasitophorous vacuole membrane was observed, similar to the construction of the cyst wall (granular region) (Fig. 5D, arrowhead).

Evaluation of structures similar to cysts after treatment with 3-BrPA of *T. gondii* in LLC-MK2 cells using fluorescence microscopy. To identify cysts in cultures during treatment with 3-BrPA, infected cells were processed for immunocytochemistry and incubated with FITC-conjugated lectin DBA. Our analysis revealed the absence of staining in control cells (Fig. 6, top panels), whereas positive staining with DBA was observed in cells treated with 3-BrPA (Fig. 6, bottom panels), indicative of the formation of cystic walls and the full establishment of cystogenesis. A quantification of positive vacuoles staining with DBA demonstrated that ~25% of vacuoles had labeling indicative of cystic walls (data not shown).

Effect of the compound atovaquone on the proliferation of *T. gondii*, RH strain, in LLC-MK2 cells. Infected cultures incubated at a parasite-to-host cell ratio of 5:1 for 1 h were washed and allowed to interact for 24 and 48 h (control group). After an infection period of 1 h, other cultures were treated for 24 and 48 h with atovaquone. The results showed that there were much fewer parasites at concentrations in the nanomolar range, with a reduction of ~51% of parasites treated for 24 h with 50 nM and a reduction of ~53% after 48 h at the same concentration (Fig. 7).

Light microscopy revealed the presence of many vacuoles with parasites in the form of rosettes in the control cultures after 24 h of interaction (Fig. 8A), whereas interactions maintained with 50 nM atovaquone treatment in the same period contained vacuoles
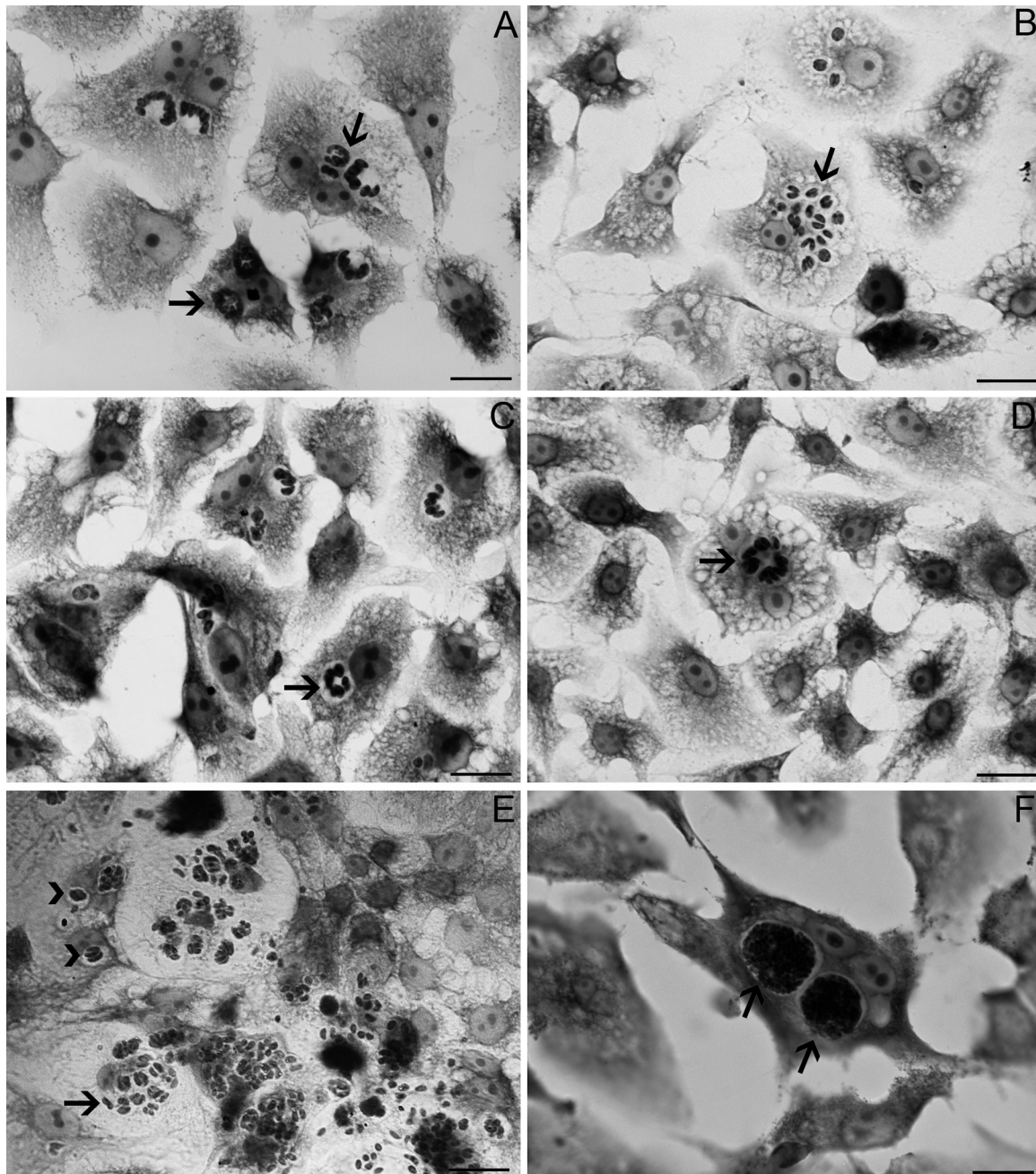
FIG 3 Light-microscopic analysis of LLC-MK2 cells infected with *T. gondii* tachyzoites after 24 h, 48 h, and 6 days using a parasite-to-host cell ratio of 5:1. (A) After 24 h, in the control group, cells with parasitophorous vacuoles containing parasites in rosette formation were noted (arrow). (B) After 24 h, cultures treated with 10 μM 3-BrPA showed fewer infected cells and cells containing parasites in pairs (arrow). (C) After 48 h of parasite-host cell interaction, the control culture presented infected cells with the same characteristics of rosette formation (arrow). (D) In the treated group, after 48 h, fewer infected cells were observed (arrow). Cultures of the control group maintained for 6 days showed lysed cells (arrow) and vacuoles containing parasites in pairs (arrowhead) (E), whereas various vacuoles containing disorganized parasites were observed (arrow) in cultures treated with 3-BrPA (F). Bars = 20 μm.

with a single parasite, indicating the absence of cell division (Fig. 8B). In interactions maintained as controls, the presence of various infected cells, most of which contained parasites arranged in rosettes, was noted after 48 h (Fig. 8C). After treatment with atovaquone, there were few infected cells, but all presented vacuoles with tachyzoites arranged in rosettes (Fig. 8D).

Effect of compound 3-BrPA with atovaquone on the proliferation of *T. gondii*, RH strain, in LLC-MK2 cells. Cultures of

LLC-MK2 cells infected with tachyzoites of *T. gondii*, RH strain, were observed for 24 and 48 h, with or without 3-BrPA, atovaquone, or 3-BrPA in combination with atovaquone. After 24 h, the cell cultures maintained with a combined treatment of 10 μM 3-BrPA and 50 nM atovaquone showed a reduced number of parasites, which represented an inhibition of ~73% compared to the number in the control cultures (Fig. 9A). This combination produced a reduction of ~49% compared with 10 μM 3-BrPA alone
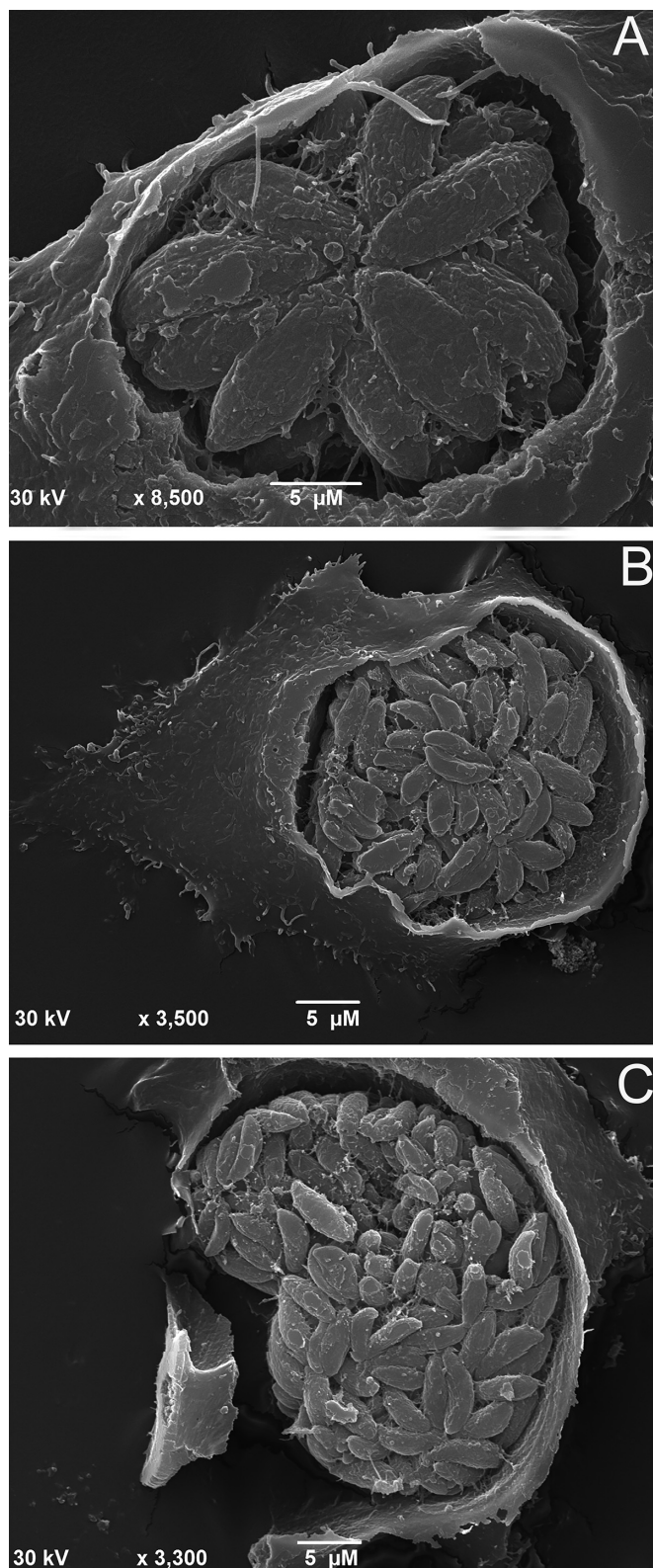
FIG 4 LLC-MK2 cells infected with *T. gondii*, RH strain, tachyzoites observed via SEM after extraction of the plasma membrane and parasitophorous vacuole membrane. (A) In the absence of treatment, parasites arranged in rosettes were observed inside the parasitophorous vacuoles. (B and C) Infected cells treated with 10 μM 3-BrPA showed structures of large volume containing many disorganized parasites, suggestive of cyst formation.

and a reduction of ~41% compared to 50 nM atovaquone (Fig. 9A).

When allowed to interact with parasites for 48 h, the cultures treated with a combination of 3-BrPA and atovaquone showed an ~71% reduction in the number of parasites compared with that in control cultures. 3-BrPA and atovaquone alone reduced parasite numbers to ~52% and ~45%, respectively (Fig. 9B).

Analysis of the presence of labeling for tachyzoites and tissue cysts in infected and treated cultures with 3-BrPA in association with atovaquone. After 6 days of interaction, LLC-MK2 cells infected with tachyzoites, RH strain, maintained without the addition of compounds showed positive staining for P30-tetramethyl rhodamine isothiocyanate (TRITC) with the presence of tachyzoites in culture and negative staining for DBA-FITC (Fig. 10A and B). In the same manner as the control, interactions maintained in the presence of 10 μM 3-BrPA and 50 nM atovaquone showed positive staining for P30-TRITC and negative staining for DBA-FITC (Fig. 10C and D).

DISCUSSION

3-Bromopyruvate, an inhibitor of cellular energy metabolism, has potent antitumor activity against different types of cancer (24). To our knowledge, this is the first study exploring the effect of 3-BrPA on the intracellular development of *T. gondii*. This study also extends work on the effect of atovaquone and the combination of both compounds on *T. gondii* interaction with LLC-MK2 cells, assessing cell proliferation and the intracellular parasite cycle under these conditions and identifying 3-BrPA as an inducer compound of cystogenesis *in vitro*.

To understand the importance of this study, it is worth recalling that *T. gondii* differentiates within the host between tachyzoites, bradyzoites, and tachyzoites and that these infectious stages have distinct physiological and biological characteristics. Mature bradyzoites are adapted for lifelong persistence in their hosts and exhibit an extreme reduction in growth rate until complete cell cycle arrest (25), with the glycolytic pathway appearing as their main source of energy. In contrast, tachyzoites, which are present during the acute phase of disease, are characterized by a rapid doubling time of 6 to 8 h, indicating that this phase is an effective pathway for the acquisition of nutrients and energy metabolism (26) and for the use of the tricarboxylic acid cycle associated with the respiratory chain to obtain energy (27) (28).

One of the initial approaches of this study was to analyze the effect of 3-BrPA on the LLC-MK2 cell line, which serves as a *T. gondii* host, to study the effect of this compound during parasite intracellular development. Our results, analyzing the proliferation of these cells during treatment, showed no effect of 3-BrPA on either the number of cells (applying the maximum compound dose used in LLC-MK2–parasite interaction studies) or cell viability, which reached 93% within 6 days. These data were expected, considering the well-known action of 3-BrPA as an inhibitor of energy metabolism on tumor cells. It was shown that 3-BrPA does not cause damage to healthy tissues in models of rabbit VX2 tumors at concentrations of 0.5 mM, a much higher concentration than we used in this study. In view of this property, this compound has been proposed as a specific anticancer agent due to its high selectivity for tumor cells (29, 30).

It is also known that tumor cell energy is derived mainly from the oxidation of glucose and that there is a substantial difference in
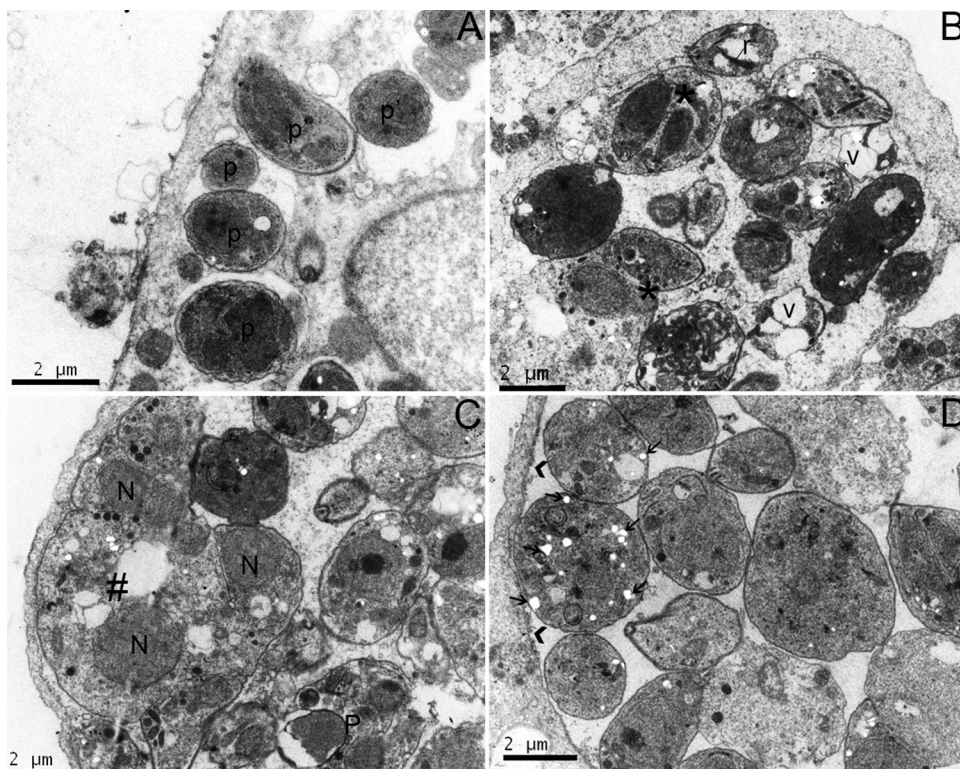
FIG 5 TEM of LLC-MK2 cells infected and maintained for 6 days of interaction. (A) Control group cells with variable numbers of vacuoles containing 1 or 2 parasites with no changes in ultrastructure (p) and parasites with good ultrastructural preservation evading from parasitophorous vacuoles were observed (p'). (B) Infected cultures maintained for 6 days treated with 10 mM 3-BrPA showed parasitophorous vacuoles with vacuolated (v) parasites, parasites with asynchronous cell division (*), and parasites with electron-dense rhoptries (r). (C) Additionally, treated cells presented anomalous structures containing vacuoles (#) with ≥2 nuclei (N) and other extremely degraded parasites (P). (D) In cultures treated with 3-BrPA, parasitophorous vacuoles contained parasites with granules similar to amylopectin (arrow), associated with an accumulation of electron-dense material in the inner face of the parasitophorous vacuole membrane (arrowhead).

glucose metabolism between normal and tumor cells, whereas glycolysis increases greatly in cancer cells (31).

In contrast, tests of 3-BrPA on the interaction of tachyzoites and LLC-MK2 cells at different concentrations showed that 3-BrPA did not affect the percentage of infected cells but was effective in controlling the intracellular proliferation of parasites, reaching 42% inhibition at a concentration of 10 μM after 24 h of exposure. The fact that there was no change in the percentage of infected cells indicates that the compound was unable to clear the infection in this period of analysis. An alternate approach to evaluate these differences was to measure the effects when the parasite-host cell ratio was varied from 3:1 to 5:1 with a single dose of 10 μM for periods of 24 h, 48 h, and 6 days. The latter approach demonstrated that the effect of the compound was both dose dependent and time dependent. Longer exposure times to 3-BrPA at concentrations of 10 μM resulted in the infection of 15% of the cells after only 48 h of interaction and 21% of the cells after 6 days. The reduction in parasite proliferation was greater at 24 and 48 h of interaction, reaching an inhibition of 55% and 61%, respectively. The selectivity of action by 3-BrPA against *Toxoplasma*, reflected in a dramatic reduction in the number of intracellular parasites in comparison with mammalian cells, may be explained by the direct biochemical evidence that the respiratory chain and oxidative phosphorylation are functional in Apicomplexa parasites, although the terminal respiratory pathway is different from the mammalian host (28).

In other protozoans, such as *Trypanosoma brucei*, the inhibitory effects of 3-BrPA on parasite motility and the efflux of pyruvate resulted in parasite death due to a blockade of the enzyme glyceraldehyde-3-phosphate dehydrogenase (GAPDH) (19, 20). It has been reported that this enzyme plays a significant role in the glycolytic flux of protozoa, such as *Leishmania mexicana*, *Plasmodium falciparum*, and *T. brucei* (32, 33). However, according to a BLAST comparison, the annotated sequence of GAPDH in *T. gondii* showed no homology with the same enzyme in *T. brucei*. On the other hand, the 3-BrPA concentrations that affected *T. brucei* were between 5.6 and 13.4 μl, which is similar to the concentration used in this study with *T. gondii*. Thus, studies are needed to relate the affinity of 3-BrPA to *T. gondii* glycolytic enzymes.

A light-microscopy analysis of cultures showed morphological differences in intracellular parasites that were mainly characterized by the presence of rosettes in the control group and a reduction in the number of parasites per vacuole, presenting primarily parasites in pairs in vacuoles and reduced numbers of infected cells in the presence of 3-BrPA. These data clearly indicate that *T. gondii* was sensitive to the action of 3-BrPA. Liu and colleagues (34) showed a new effect of 3-BrPA that, at least in MCF-7 breast cancer cells, the compound inhibits cell proliferation by inhibiting the S and G$_2$/M phases of the cycle cell, promoting apoptosis in these cells. We have accumulated evidence that the compound is capable of interfering in the process of endodyogeny, generating cell bodies of large volume containing various organelles, which
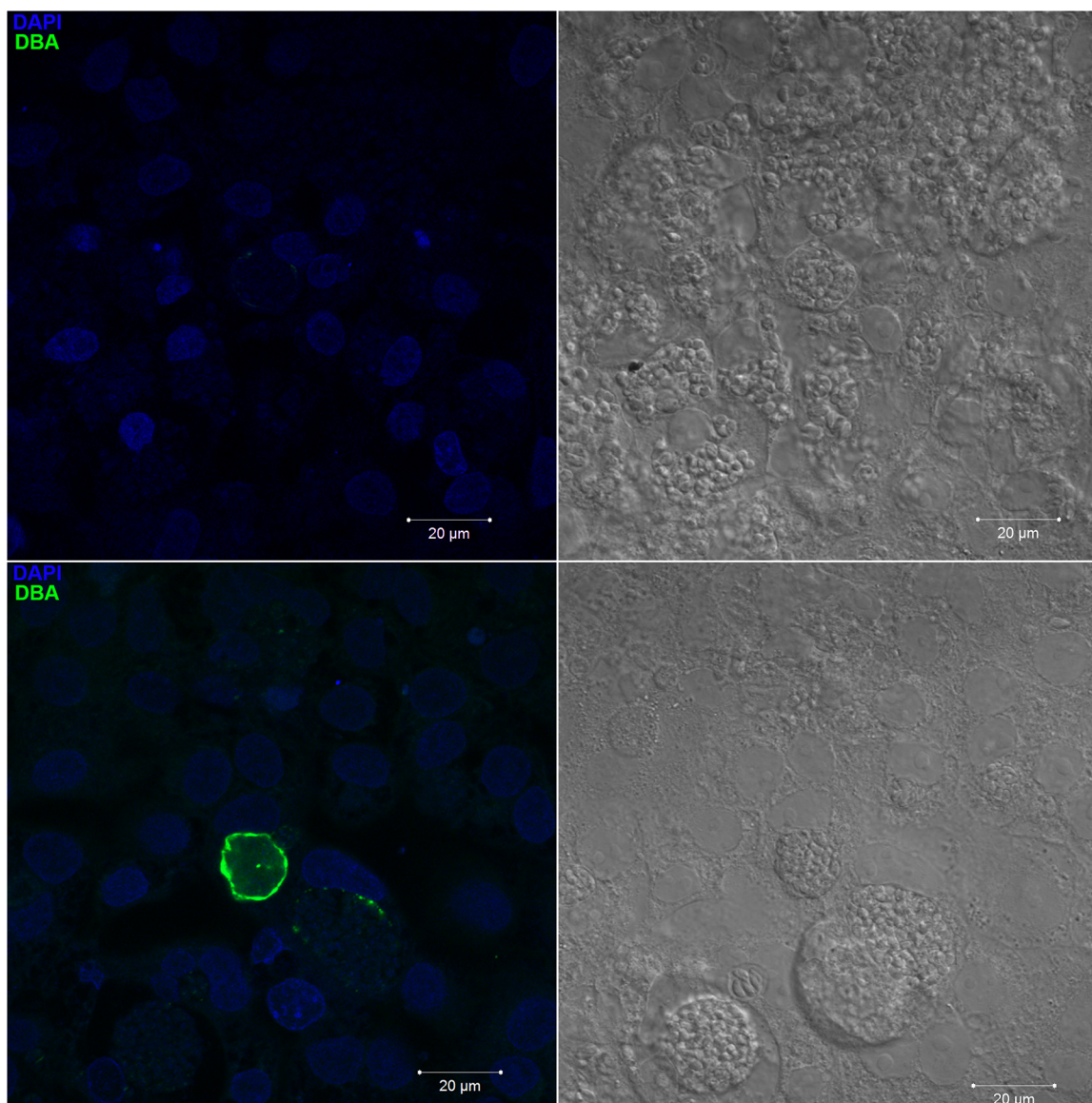
FIG 6 LLC-MK2 cells infected with *T. gondii*, RH strain, tachyzoites incubated with FITC-conjugated DBA. Control experiment, without treatment, showed no marking DBA (top panels). After treatment with 10 μM 3-BrPA, the cyst wall was shown via positive staining with DBA-FITC (bottom left) and differential interferential microscopy (DIC) (bottom right). Fluorescence microscopy staining with DAPI revealed cell nuclei (left panels). DIC showed intracellular parasites (right panels).

are multinucleate and disorganized structures with incomplete endodyogeny (Fig. 5C). Similar images have been described by Martins-Duarte et al. (35) using itraconazole against *T. gondii*. This observation leads to the idea that the number of intracellular parasites decreases due to both endodyogeny-independent cell death and a blockade of cytokinesis during cell division, which may be analogous to the inhibition of mammalian cell proliferation that triggers apoptosis, as proposed by Liu et al. (34).

Initially, blocking of cell proliferation was indicated by (i) the reduction of intracellular parasites according to quantitative analysis; (ii) the visualization of low numbers of rosettes, which suggested low endodyogeny activity; and (iii) images acquired via TEM clearly showing that 3-BrPA did not affect all parasites within the same culture, cell, or vacuole (Fig. 5B to D). Different
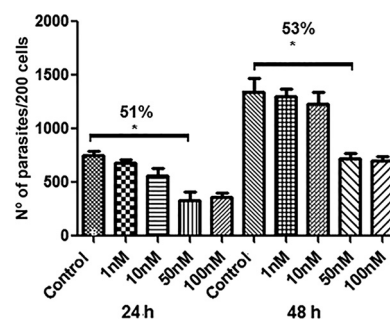

FIG 7 LLC-MK2 cells infected with *T. gondii*, RH strain at a parasite-to-host cell ratio of 5:1 after treatment with atovaquone in different concentrations at 24 and 48 h of infection. *, $P \leq 0.05$.
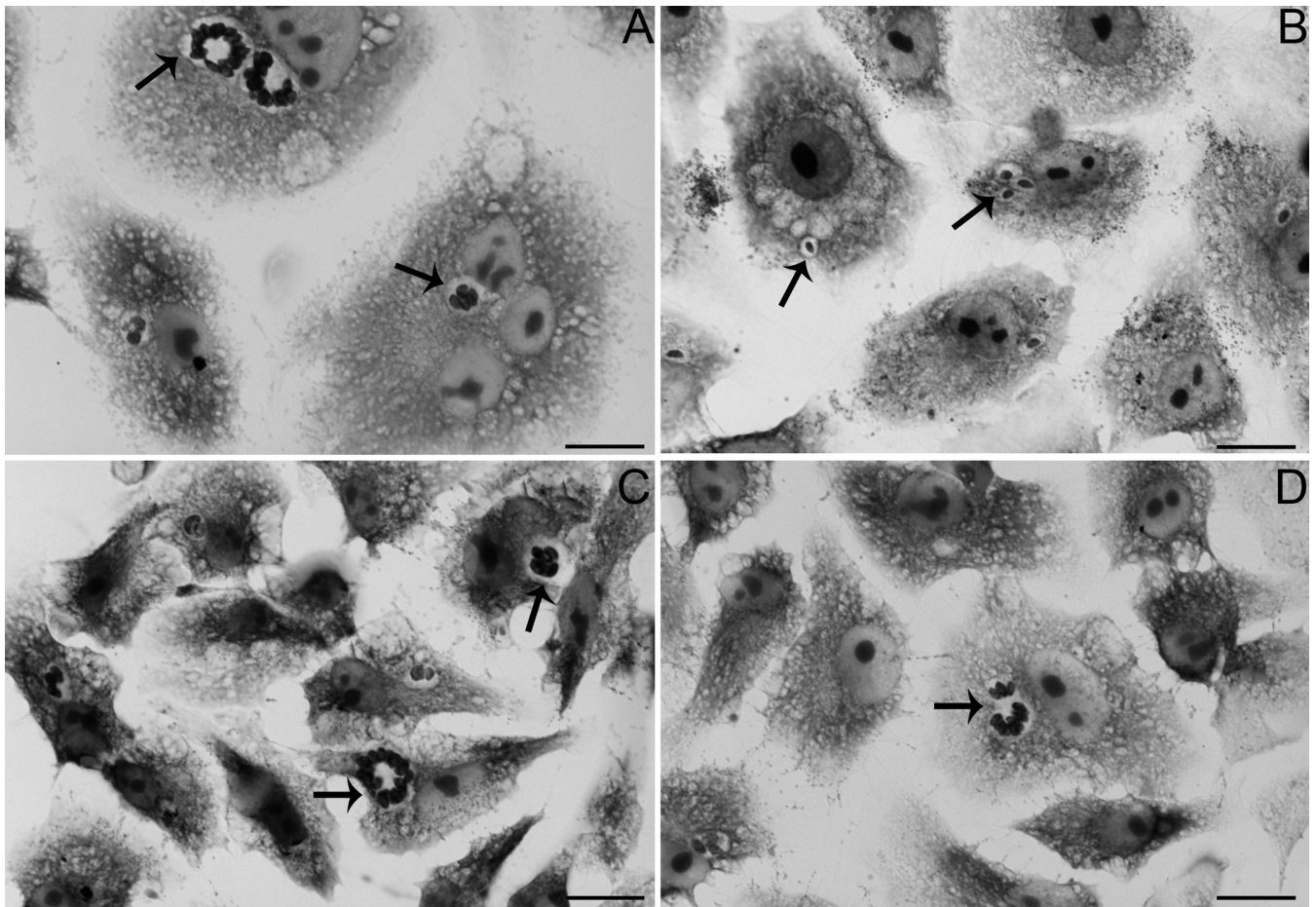
FIG 8 LLC-MK2 cells infected with *T. gondii*, RH strain, at a parasite-to-host cell ratio of 5:1 observed via light microscopy. After 24 h of infection, more parasites per vacuole were noted in cultures maintained without treatment (A) than in cultures maintained on treatment with 50 and 100 nM atovaquone (B). After 48 h, the control group showed parasites in a rosette arrangement and a greater number of parasites in each vacuole (C). In contrast, cultures maintained on treatment with 50 and 100 nM atovaquone showed fewer infected cells and parasites per vacuole (D). Bar = 20 μm.
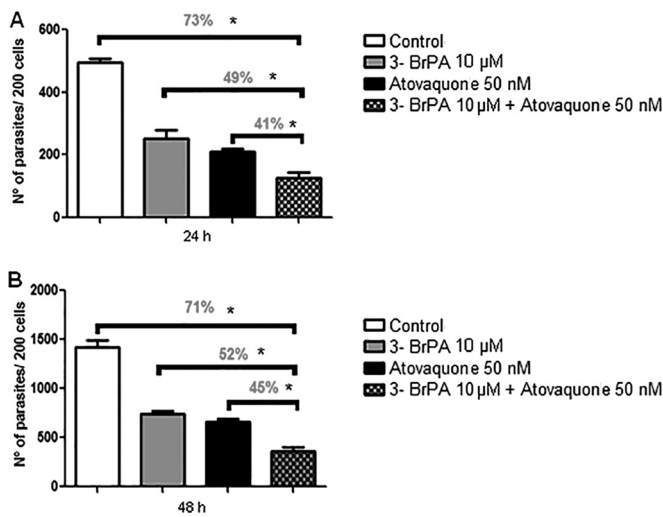

FIG 9 Culture cells infected with *T. gondii*, RH strain, at a parasite-to-host cell ratio of 5:1 under different treatments. Cultures maintained on treatment with atovaquone, 3-BrPA, and atovaquone in combination with 3-BrPA for 24 h (A) and 48 h (B) of treatment. *, $P \leq 0.05$.

morphological stages in the same vacuole, including parasites with good preservation and others with classic features of cell death, were observed. We did not investigate whether the compound stimulated cell death by apoptosis or autophagy, but such assumptions cannot be discarded in view of the studies that demonstrate the induction of these pathways as an effect of 3-BrPA (34, 36–38).

Another observation obtained in the course of monitoring the infection was that 3-BrPA was able to induce the formation of cysts in cells infected with tachyzoites. This finding was supported by (i) the presence of parasitophorous vacuoles with large amounts of unorganized parasites, as observed using light microscopy of stained cultures with Giemsa and SEM; (ii) the revelation of cystic walls via an incubation of cultures with lectin DBA, which recognizes and binds in GalNAc residues, indicating that the process of cystogenesis had been established in cells treated with 3-BrPA; (iii) the presence of granules similar to the amylopectin granules present in bradyzoites; and (iv) the thickness of parasitophorous vacuole membranes, indicating a modification of this membrane for the construction of the cyst wall. The LLC-MK2 cell line used in this work has been used during the infection of tachyzoites of different strains, demonstrating that the EGS strain (Brazilian strain of type II)
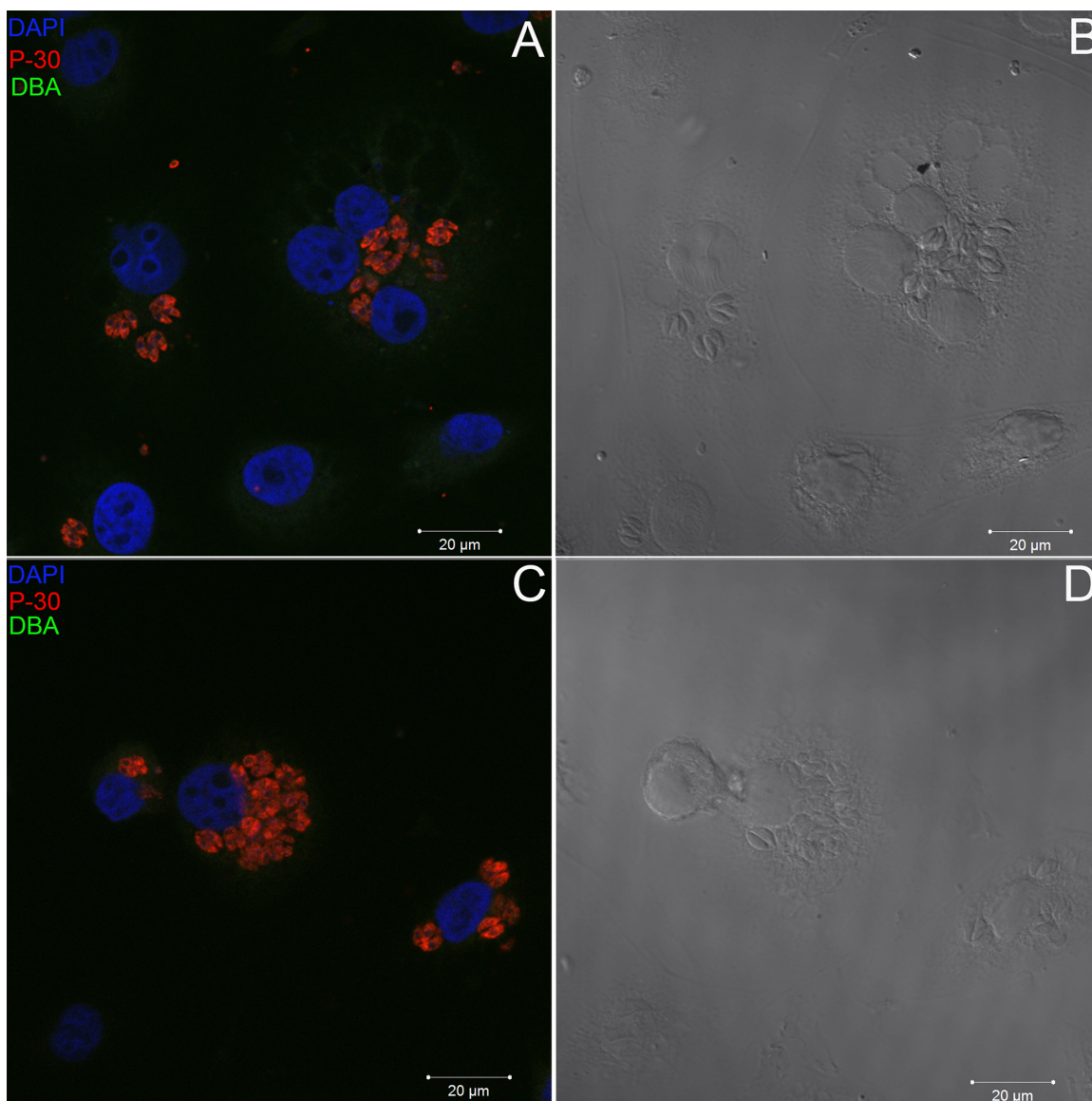
FIG 10 LLC-MK2 cells infected with *T. gondii* after 6 days of treatment with 10 μM 3-BrPA in combination with 50 nM atovaquone. These cells were incubated with anti-P30 and DBA-FITC, revealing only tachyzoites stained in red. Control (A) and treated (C) cells are shown. Nuclei were labeled with DAPI (blue). Differential interference contrast microscopy images are shown in panels B and D.

establishes cystogenesis in these cells spontaneously, with rates of almost 80% (39). In contrast, the same researchers demonstrated that tachyzoites of the RH strain (type I) showed a low conversion capacity (~4% in 96 h). These data are similar to results previously obtained with skeletal muscle cells (conversion in 3% of vacuoles), in which the conversion was already established after 18 h of interaction (40). Thus, our results showing a 25% induction of cystogenesis by 3-BrPA reinforces the role of this compound in cellular events.

One of the known mechanisms of action of 3-BrPA is blockage of the glycolytic pathway in tumor cells (24). A demonstration that the infected cells treated with the compound induced cystogenesis suggests that this route may also be blocked in *T. gondii*. The understanding of this process leads us to suggest that the induction of cystogenesis may have been triggered by the parasite; as an alternative, this blockage may use nutrients from other metabolic pathways. In this case, another alternative to obtain energy for the parasite would be by the tricarboxylic acid pathway, using acyl-CoA, formed in the breakdown of fatty acids, to generate ATP. Therefore, we hypothesize that when this compound blocked the glycolytic pathway, the parasite, under metabolic stress, used this alternative pathway, and the genes responsible for modulation of cystogenesis were activated, as demonstrated by the presence of the cystic wall following treatment. A confirmation of this hypothesis may advance our knowledge of *T. gondii* metabolic processes.

Treatment of the infected cell cultures with atovaquone in combination with 3-BrPA potentiated the effect of the compounds alone, suggesting that blockage of the glycolytic pathway of *T. gondii* by 3-BrPA and the oxidative phosphorylation induced

by atovaquone may suppress cystogenesis. This study demonstrated that use of these compounds in combination was more efficient in eliminating the parasite than either compound alone. The combination led to fewer parasite-infected cells with no evidence of cystogenesis. However, the infection was not completely eliminated, possibly because there are other ways for the parasite to obtain energy, for example, via the apicoplast. This organelle is important in *T. gondii* metabolism, as it is the site of the biosynthesis of fatty acid type II, isoprenoids, and some enzymes of carbohydrate metabolism (26, 41–43). Inclusion of the apicoplast as an alternate route of cellular respiration of the parasite was considered in a study by Fleige et al. (26) that located several key enzymes of *T. gondii* carbohydrate metabolism in the cytosol and the apicoplast of the parasites. The cytoplasm has a complete set of enzymes for glycolysis, which should allow the parasite to metabolize glucose. Genes for all glycolytic enzymes, phosphofructokinase, and pyruvate kinase are present in the *T. gondii* genome, and multiple copies and isoforms of triose phosphate isomerase, phosphoglycerate kinase, and pyruvate kinase are located exclusively in the apicoplast. The mRNA expression levels of all genes with glycolytic products were compared between tachyzoites and bradyzoites, but a specific expression pattern was observed in only bradyzoites for enolase I. The *T. gondii* genome encodes a single complex of pyruvate dehydrogenase, which was located in the apicoplast and is absent in mitochondria. An exchange of metabolites between the cytosol and apicoplast is most likely mediated by a phosphate translocator, which was present in the apicoplast. Thus, results obtained in this study support those of Fleige et al. (26), who proposed a model that would explain the supply of ATP by the apicoplast, as well as the exchange of metabolites between the cytosol and apicoplast.

The data set obtained in this work demonstrates that there are gaps in our knowledge of *T. gondii* metabolism and its importance for cystogenesis. Moreover, it suggests that 3-BrPA may be a good tool for the study of cystogenesis *in vitro* and for the study of *T. gondii* metabolism.

ACKNOWLEDGMENTS

REFERENCES

1. **Tenter AM, Heckeroth AR, Weiss LM.** 2000. *Toxoplasma gondii*: from animals to human. Int J Parasitol **30:**1217–1258. http://dx.doi.org/10.1016/S0020-7519(00)00124-7.
2. **Black MW, Boothroyd JC.** 2000. Lytic cycle of *Toxoplasma gondii*. Microbiol Mol Biol Rev **64:**607–623. http://dx.doi.org/10.1128/MMBR.64.3.607-623.2000.
3. **Montoya JG, Liesenfeld O.** 2004. Toxoplasmosis. Lancet **363:**1965–1976. http://dx.doi.org/10.1016/S0140-6736(04)16412-X.
4. **Diniz EMA, Vaz FAC.** 2003. Qual é a recomendação atual para o tratamento da toxoplasmose congênita? Rev Assoc Med Bras **49:**10. http://dx.doi.org/10.1590/S0104-42302003000100016.
5. **Baggish AL, Hill DR.** 2002. Antiparasitic agent atovaquone. Antimicrob Agents Chemother **46:**1163–1173. http://dx.doi.org/10.1128/AAC.46.5.1163-1173.2002.
6. **Romand S, Della Bruna C, Farinotti R, Derouin F.** 1996. *In vitro* and *in vivo* effects of rifabutin alone or combined with atovaquone against *Toxoplasma gondii*. Antimicrob Agents Chemother **40:**2015–2020.
7. **Meneceur P, Bouldouyre MA, Aubert D, Villena I, Menotti J, Sauvage V, Garin JF, Derouin F.** 2008. *In vitro* susceptibility of various genotypic strains of *Toxoplasma gondii* to pyrimethamine, sulfadiazine, and atovaquone. Antimicrob Agents Chemother **52:**1269–1277. http://dx.doi.org/10.1128/AAC.01203-07.
8. **Djurković-Djaković O, Nikolić T, Robert-Gangneux F, Bobić B, Nikolić A.** 1999. Synergistic effect of clindamycin and atovaquone in acute murine toxoplasmosis. Antimicrob Agents Chemother **43:**2240–2244.
9. **Ko YH, Smith BL, Wang Y, Pomper MG, Rini DA, Torbenson MS.** 2004. Advanced cancers: eradication in all cases using 3-bromopyruvate therapy to deplete ATP. Biochem Biophys Res Commun **324:**269–275. http://dx.doi.org/10.1016/j.bbrc.2004.09.047.
10. **Kim W, Yoon JH, Jeong JM, Cheon GJ, Lee TS, Yang JI.** 2007. Apoptosis-inducing antitumor efficacy of hexokinase II inhibitor in hepatocellular carcinoma. Mol Cancer Ther **6:**2554–2562. http://dx.doi.org/10.1158/1535-7163.MCT-07-0115.
11. **Cardaci S, Desideri E, Ciriolo MR.** 2012. Targeting aerobic glycolysis: 3-bromopyruvate as a promising anticancer drug. J Bioenerg Biomembr **44:**17–29. http://dx.doi.org/10.1007/s10863-012-9422-7.
12. **Ko YH, Pedersen PL, Geschwind JF.** 2001. Glucose catabolism in the rabbit VX2 tumor model for liver cancer: characterization and targeting hexokinase. Cancer Lett **173:**83–91. http://dx.doi.org/10.1016/S0304-3835(01)00667-X.
13. **Shoshan MC.** 2012. 3-Bromopyruvate: targets and outcomes. J Bioenerg Biomembr **44:**7–15. http://dx.doi.org/10.1007/s10863-012-9419-2.
14. **El Sayed SM, Mohamed WG, Seddik MA, Ahmed AS, Mahmoud AG, Amer WH, Helmy Nabo MM, Hamed AR, Ahmed NS, Abd-Allah AA.** 2014. Safety and outcome of treatment of metastatic melanoma using 3-bromopyruvate: a concise literature review and case study. Chin J Cancer **33:**356–364.
15. **Pereira da Silva AP, El-Bacha T, Kyaw N, dos Santos RS, da-Silva WS, Almeida FC, Da Poian AT, Galina A.** 2009. Inhibition of energy-producing pathways of HepG2 cells by 3-bromopyruvate. Biochem J **417:**717–726. http://dx.doi.org/10.1042/BJ20080805.
16. **Ganapathy-Kanniappan S, Geschwind JF, Kunjithapatham R, Buijs M, Vossen JA, Tchernyshyov I, Cole RN, Syed LH, Rao PP, Ota S, Vali M.** 2009. Glyceraldehyde-3-phosphate dehydrogenase (GAPDH) is pyruvylated during 3-bromopyruvate mediated cancer cell death. Anticancer Res **29:**4909–4918.
17. **Lis P, Zarzycki M, Ko YK, Casal M, Pedersen PL, Goffeau A, Ułaszewski S.** 2012. Transport and cytotoxicity of the anticancer drug 3-bromopyruvate in the yeast *Saccharomyces cerevisiae*. J Bioenerg Biomembr **44:**155–161. http://dx.doi.org/10.1007/s10863-012-9421-8.
18. **Dylag M, Lis P, Niedzwiecka K, Ko YH, Pedersen PL, Goffeau A, Ułaszewski S.** 2013. 3-Bromopyruvate: a novel antifungal agent against the human pathogen *Cryptococcus neoformans*. Biochem Biophys Res Commun **434:**322–327. http://dx.doi.org/10.1016/j.bbrc.2013.02.125.
19. **Barnard JP, Reynafarje B, Pedersen PL.** 1993. Glucose catabolism in African trypanosomes: evidence that the terminal step is catalyzed by a pyruvate transporter capable of facilitating uptake of toxic analogs. J Biol Chem **268:**3654–3661.
20. **Vanderheyden N, Wong J, Docampo R.** 2000. A pyruvate–proton symport and an H+-ATPase regulate the intracellular pH of *Trypanosoma brucei* at different stages of its life cycle. Biochem J **346:**53–62. http://dx.doi.org/10.1042/0264-6021:3460053.
21. **Zhang YW, Halonen SK, Ma YF, Wittner M, Weiss LM.** 2001. Initial characterization of CST1, a *Toxoplasma gondii* cyst wall glycoprotein. Infect Immun **69:**501–507.
22. **Flood PP.** 1975. Scanning electron microscope observations on the muscle innervation of *Oikopleura dioica* Fol (Appendicularia, Tunicata) with notes on the arrangement of connective tissue fibres. Cell Tissue Res **164:**357–369.
23. **De Souza W, Campanati L, Attias M.** 2008. Strategies and results of field emission scanning electron microscopy (FE-SEM) in the study of parasitic

protozoa. Micron **39**:77–87. http://dx.doi.org/10.1016/j.micron.2006.11
.003.

24. **Pedersen PL.** 2012. 3-Bromopyruvate (3BP) a fast acting, promising, powerful, specific, and effective "small molecule" anti-cancer agent taken from labside to bedside: introduction to a special issue. J Bioenerg Biomembr **44**:1–6. http://dx.doi.org/10.1007/s10863-012-9425-4.

25. **Dubey JP, Lindsay DS, Speer CA.** 1998. Structures of *Toxoplasma gondii* tachyzoites, bradyzoites, and sporozoites and biology and development of tissue cysts. Clin Microbiol Rev **11**:267–299.

26. **Fleige T, Fischer K, Ferguson DJ, Gross U, Bohne W.** 2007. Carbohydrate metabolism in the *Toxoplasma gondii* apicoplast: localization of three glycolytic isoenzymes, the single pyruvate dehydrogenase complex, and a plastid phosphate translocator. Eukaryot Cell **6**:984–996. http://dx .doi.org/10.1128/EC.00061-07.

27. **Denton H, Roberts CW, Alexander J, Thong KW, Coombs GH.** 1996. Enzymes of energy metabolism in the bradyzoites and tachyzoites of *Toxoplasma gondii*. FEMS Microbiol Lett **137**:103–108. http://dx.doi.org/10 .1111/j.1574-6968.1996.tb08090.x.

28. **Vercesi A, Rodrigues CO, Uyemura AS, Zhong L, Moreno SNJ.** 1998. Respiration and oxidative phosphorylation in the Apicomplexan parasite *Toxoplasma gondii*. J Biol Chem **273**:31040–31047. http://dx.doi.org/10 .1074/jbc.273.47.31040.

29. **Nelson K.** 2002. 3-Bromopyruvate kills cancer cells in animals. Lancet Oncol **3**:524. http://dx.doi.org/10.1016/S1470-2045(02)00867-7.

30. **Geschwind JF, Ko YH, Torbenson MS, Magee C, Pedersen PL.** 2002. Novel therapy for liver cancer: direct intraarterial injection of a potent inhibitor of ATP production. Cancer Res **62**:3909–3913.

31. **Pedersen PL.** 2007. Warburg, me and hexokinase 2: multiple discoveries of key molecular events underlying one of cancers' most common phenotypes, the "Warburg effect," i.e., elevated glycolysis in the presence of oxygen. J Bioenerg Biomembr **39**:211–222. http://dx.doi.org/10.1007 /s10863-007-9094-x.

32. **Vellieux FM, Hajdu J, Verlinde CL, Groendijk H, Read RJ, Greenhough TJ, Campbell JW, Kalk KH, Littlechild JA, Watson HC.** 1993. Structure of glycosomal glyceraldehyde-3-phosphate dehydrogenase from *Trypanosoma brucei* determined from Laue data. Proc Natl Acad Sci U S A **90**: 2355–2359. http://dx.doi.org/10.1073/pnas.90.6.2355.

33. **Satchell JF, Malby RL, Luo CS, Adisa A, Alpyurek AE, Klonis N, Smith BJ, Tilley L, Colman PM.** 2005. Structure of glyceraldehyde-3-phosphate dehy-

drogenase from *Plasmodium falciparum*. Acta Crystallogr D-Biol Crystallogr **61**:1213–1221. http://dx.doi.org/10.1107/S0907444905018317.

34. **Liu XH, Zheng XF, Wang YL.** 2009. Inhibitive effect of 3-bromopyruvic acid on human breast cancer MCF-7 cells involves cell cycle arrest and apoptotic induction. Chin Med J (Engl) **122**:1681–1685.

35. **Martins-Duarte ES, de Souza W, Vommaro RC.** 2008. Itraconazole affects *Toxoplasma gondii* endodyogeny. FEMS Microbiol Lett **282**:290–298. http://dx.doi.org/10.1111/j.1574-6968.2008.01130.x.

36. **Egger L, Schneider J, Rheme C, Tapernoux M, Hacki J, Borner C.** 2003. Serine proteases mediate apoptosis-like cell death and phagocytosis under caspase-inhibiting conditions. Cell Death Differ **10**:1188–1203. http://dx .doi.org/10.1038/sj.cdd.4401288.

37. **Xu C, Bailly-Maitre B, Reed JC.** 2005. Endoplasmic reticulum stress: cell life and death decisions. J Clin Invest **115**:2656–2664. http://dx.doi.org/10 .1172/JCI26373.

38. **Ganapathy-Kanniappan S, Geschwind JF, Kunjithapatham R, Buijs M, Syed LH, Rao PP, Ota S, Kwak BK, Loffroy R, Vali M.** 2010. 3-Bromopyruvate induces endoplasmic reticulum stress, overcomes autophagy and causes apoptosis in human HCC cell lines. Anticancer Res **30**:923–935.

39. **Paredes-Santos TC, Martins-Duarte ES, Vitor RW, de Souza W, Attias M, Vommaro RC.** 2013. Spontaneous cystogenesis *in vitro* of a Brazilian strain of *Toxoplasma gondii*. Parasitol Int **62**:181–188. http://dx.doi.org/10 .1016/j.parint.2012.12.003.

40. **Ferreira-da-Silva MF, Rodrigues RM, Andrade EF, Carvalho L, Gross U, Lüder CGK, Barbosa HS.** 2009. Spontaneous stage differentiation of mouse-virulent *Toxoplasma gondii* RH parasites in skeletal muscle cells: an ultrastructural evaluation. Mem Inst Oswaldo Cruz **104**:196–200. http: //dx.doi.org/10.1590/S0074-02762009000200012.

41. **Kohler S, Delwiche CF, Denny PW, Tilney LG, Webster P, Wilson RJ, Roos DS.** 1997. A plastid of probable green algal origin in Apicomplexan parasites. Science **275**:1485–1489. http://dx.doi.org/10.1126/science.275.5305.1485.

42. **Gleeson MT.** 2000. The plastid in Apicomplexa: what use is it? Int J Parasitol **30**:1053–1070. http://dx.doi.org/10.1016/S0020-7519(00)00100-4.

43. **Mazumdar J, Wilson EH, Masek K, Hunter CA, Striepen B.** 2006. Apicoplast fatty acid synthesis is essential for organelle biogenesis and parasite survival in *Toxoplasma gondii*. Proc Natl Acad Sci U S A **103**: 13192–12197. http://dx.doi.org/10.1073/pnas.0603391103.